Measurements of the Decays $\phi \to \eta\gamma$, $\pi^0\gamma$, $\eta'\gamma$ at SND.

M.N. Achasov, A.V. Berdyugin, A.V. Bozhenok, D.A. Bukin, S.V. Burdin, T.V. Dimova, V.P. Druzhinin, M.S. Dubrovin, I.A. Gaponenko, V.B. Golubev, V.N. Ivanchenko, A.A. Korol, S.V. Koshuba, E.V. Pakhtusova, A.A. Salnikov[a], S.I. Serednyakov, V.V. Shary, Z.K. Silagadze

[a]Corresponding author, e-mail: salnikov@inp.nsk.su

We present the results of the studies of radiative decays of ϕ meson into $\eta\gamma$, $\pi^0\gamma$ and $\eta'\gamma$ final states, performed in SND experiment at the VEPP-2M collider. The following values for the decay probabilities were obtained $B(\phi \to \eta\gamma) = (1.338 \pm 0.012 \pm 0.052)\%$ for $\eta \to \gamma\gamma$ decay mode, $B(\phi \to \eta\gamma) = (1.29 \pm 0.02 \pm 0.057)\%$ for $\eta \to 3\pi^0$ decay mode, $B(\phi \to \pi^0\gamma) = (1.173 \pm 0.033^{+0.12}_{-0.10}) \times 10^{-3}$, and $B(\phi \to \eta'\gamma) = (6.7^{+3.3}_{-2.9}) \times 10^{-5}$.

1. Introduction

The studies of the radiative decays of light vector mesons (ρ, ω, ϕ) in e^+e^- collisions play an important role in understanding of the electromagnetic structure of $q\bar{q}$-states and low-energy behavior of strong interactions [1–3]. With the beginning of CMD-2 [4] and SND [5,6] experiments at the VEPP-2M collider, a new opportunity emerges to increase significantly experimental statistics and reduce the uncertainties of the observed results.

In this work we present the results of studies of the processes $e^+e^- \to \eta\gamma$, $\pi^0\gamma$, and $\eta'\gamma$ in the ϕ-meson region, which were obtained with the experimental data gathered in the SND experiment. Previous information on these processes is mainly from the e^+e^- experiments ND [7], and CMD-2 [8–10], performed also at VEPP-2M.

2. Detector SND and experiment

SND is a general-purpose non-magnetic detector [5] designed and optimized for the observation of neutral particles. The main part of the detector is an electromagnetic calorimeter built of 1632 NaI(Tl) crystals. Full thickness of the calorimeter for the particles originating from the interaction point is $13.5X_0$. The calorimeter provides a good energy resolution for photons, which can be approximated as $\sigma_E(E)/E = 4.2\%/E(GeV)^{1/4}$ [11]. An angular resolution is determined primarily by the size of the crystals and is approximately equal to $\sigma_{\theta,\varphi} = 1.5°$ [12]. The calorimeter and the event reconstruction program allow to detect photons with the energies above 20 MeV with a solid angle coverage 90% of 4π.

The experiments with the SND detector were carried out at the VEPP-2M collider with the average luminosity $\sim 10^{30}$ cm^{-2}sec^{-1}. In this work we present the results based on the experimental statistics collected during 1996 year, which includes 7 scans of the energy region 985–1040 MeV. Total integrated luminosity accumulated in these scans is 4.3 pb^{-1}, corresponding to approximately 8.2×10^6 events of ϕ meson decays.

3. Decays $\phi \to \eta\gamma$, $\pi^0\gamma \to 3\gamma$

Two radiative decays $\phi \to \eta\gamma$ and $\phi \to \pi^0\gamma$ were studied in 3-gamma final state in the processes $e^+e^- \to \eta\gamma, \pi^0\gamma \to \gamma\gamma\gamma$. The main background is coming from non-resonant QED three-quanta annihilation $e^+e^- \to \gamma\gamma\gamma$, and from the two-quanta annihilation with the appearance of additional spurious hits in the calorimeter.

The analysis of the data was performed in two stages. The pre-selection imposed following conditions: (1) presence of three or four reconstructed photons, (2) total energy deposition in the calorimeter ($E_{\rm tot}$) is in the range from $0.7\sqrt{s}$ to $1.2\sqrt{s}$, where $s = 4E^2_{\rm beam}$, (3) the absolute value of the sum of the momenta of all particles is lower than $0.2E_{\rm tot}/c$, (4) minimal energy of the photons is 50 MeV; polar angle for the photons with energies 50–100 MeV is in the range $45° < \theta < 135°$, for the photons with the energies higher than 100 MeV — $27° < \theta < 153°$. The last condition was introduced to suppress the spurious hits in the calorimeter, which appear mainly in the crystals closest to the beam. The number of events, which passed this preliminary selection, was about 139 000.

Further selection was based on the kinematic fit of the events. Employing the 4-momentum conservation it is possible with this procedure to build statistical tests for the different intermediate states in the observed event. For each event the following four hypotheses were tested:

1. hypothesis $H_{2\gamma}$: two most energetic photons are due to the process $e^+e^- \to \gamma\gamma$. This hypothesis was used for the further suppression of spurious signals in the

calorimeter,

2. hypothesis $H_{3\gamma}$: three photons in the event are from the process $e^+e^- \to \gamma\gamma\gamma$ (QED),
3. hypothesis $H_{\eta\gamma}$: three photons in the event are from the process $e^+e^- \to \eta\gamma \to \gamma\gamma\gamma$,
4. hypothesis $H_{\pi\gamma}$: three photons in the event are from the process $e^+e^- \to \pi^0\gamma \to \gamma\gamma\gamma$.

One can notice that the hypotheses $H_{\eta\gamma}$ and $H_{\pi\gamma}$ are similar to the hypothesis $H_{3\gamma}$, but have the additional constraint on the invariant mass of the pair of photons. For the further analysis only the events which satisfy the $H_{3\gamma}$ hypothesis but do not satisfy the $H_{2\gamma}$ hypothesis were selected. These events were divided further into 4 non-overlapping classes using the hypotheses $H_{\eta\gamma}$ and $H_{\pi\gamma}$:

A. events satisfying hypothesis $H_{\eta\gamma}$ but not $H_{\pi\gamma}$,

B. events satisfying hypothesis $H_{\pi\gamma}$ but not $H_{\eta\gamma}$,

C. events satisfying both hypotheses $H_{\eta\gamma}$ and $H_{\pi\gamma}$,

D. events not satisfying any of the hypotheses $H_{\eta\gamma}$ and $H_{\pi\gamma}$.

Classes A and B contain events of the processes $e^+e^- \to \eta\gamma$ and $e^+e^- \to \pi^0\gamma$ respectively, with some small admixture of events $e^+e^- \to \gamma\gamma\gamma$ (QED). Class D contains events of process $e^+e^- \to \gamma\gamma\gamma$ (QED), while class C contains events from all three processes.

The expected number of events for each selection class in one energy point was approximated by the dependence

$$N_q^{th}(E) = L(E) \times \sum_p \sigma_p(E)\beta_p(E)\varepsilon_{q,p}(E), \qquad (1)$$

where $N_q^{th}(E)$ is the expected number of events in the selection class q, $L(E)$ is the integrated luminosity in the energy point, $\sigma_p(E)$ is a cross-section of the process p, $\beta_p(E)$ is a factor taking into account radiative corrections [13] and a beam energy spread, $\varepsilon_{q,p}(E)$ is an efficiency of the selection algorithm for the process p in the selection class q. Summation is performed over the three main processes — $e^+e^- \to \eta\gamma$, $e^+e^- \to \pi^0\gamma$ and $e^+e^- \to \gamma\gamma\gamma$, a contribution from other processes, both resonant and non-resonant, estimated from the full simulation, is negligible.

For the description of the cross-section of processes $e^+e^- \to P\gamma$, where P is a pseudoscalar meson, the following dependence was used:

$$\sigma(s) = \frac{F(s)}{s^{3/2}} \left| \sum_{V=\rho,\omega,\phi} A_V(s) \right|^2, \qquad (2)$$

$$A_V(s) = \sqrt{\sigma_{VP\gamma} \frac{m_V^3}{F(m_V^2)}} \frac{m_V \Gamma_V e^{i\varphi_V}}{m_V^2 - s - i\sqrt{s}\Gamma_V(s)},$$

where $\sigma_{VP\gamma} = 12\pi B(V \to e^+e^-)B(V \to P\gamma)/m_V^2$ is the cross section of the process $e^+e^- \to V \to P\gamma$ at the maximum of vector resonance V. $F(s)$ is the phase space factor for the process $e^+e^- \to P\gamma$. Phases of vector mesons were taken to be $\varphi_\rho = \varphi_\omega = 0$, $\varphi_\phi = 180°$ for $\eta\gamma$ decay, $\varphi_\phi = (158 \pm 11)°$ for $\pi^0\gamma$ decay.

The cross section of the process $e^+e^- \to \gamma\gamma\gamma$ was described using the formulae from ref. [14], which do not take into account the radiative corrections. The factor β_p in eq. (1) for this process was determined from the fit of the experimental data of the selection class D.

Parameters of the decays $\phi \to \eta\gamma$ and $\phi \to \pi^0\gamma$ were determined from the simultaneous fit of the expected number of events to the number of the observed events in selection classes A, B, and C. Fig. 1 represents the registration cross section, $\sigma_{\rm vis} = N/L$, in selection classes A and B for all experimental points together with the theoretical curves obtained from the fit. Using the table values of $B(\phi \to e^+e^-)$, $B(\eta \to \gamma\gamma)$ and $B(\pi^0 \to \gamma\gamma)$ [15] we obtain the following values from the fit:

$$B(\phi \to \eta\gamma) = (1.338 \pm 0.012 \pm 0.052)\%, \quad (3)$$

$$B(\phi \to \pi^0\gamma) = (1.226 \pm 0.036^{+0.096}_{-0.089}) \times 10^{-4} \quad (4)$$

In the quoted errors the first represent a statistical error, and the second – systematic. The main contributors to the systematic errors are uncertainties in the integrated luminosity (2.5%), in the efficiency evaluation (1–2%), and in the values $B(\phi \to e^+e^-)$ (3%) and $B(\eta \to \gamma\gamma)$ (1%). For the decay $\pi^0\gamma$ the uncertainty in the phase φ_ϕ was also included in the systematic error (6%). In the determination of the partial widths of decays $\phi \to \eta\gamma$ and $\phi \to \pi^0\gamma$ some of the systematic effects are common to both, hence in their ratio the errors caused by these effects cancel: $\Gamma(\phi \to \eta\gamma)/\Gamma(\phi \to \pi^0\gamma) = 10.9 \pm 0.3^{+0.7}_{-0.8}$.

4. Decay $\phi \to \eta\gamma \to 3\pi^0\gamma$

The same decay $\phi \to \eta\gamma$ was studied in the different final state when η decays into three π^0 [16]. The characteristic feature of this process, used in the analysis, is a fixed value of the energy of recoil gamma. The events with 6 to 8 registered photons were selected for the analysis. The standard SND cuts [17] for the energy-momentum balance were applied to this events, which eliminate the cosmic background and suppress the main background process $e^+e^- \to \phi \to K_S K_L \to \pi^0\pi^0 K_L$. The total number of selected events is about

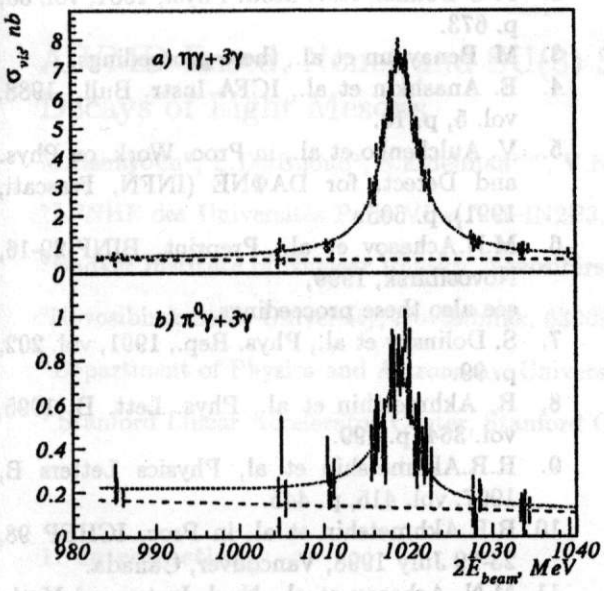

Figure 1. Registration cross section for the selection classes A (plot a) and B (plot b). Curves represent fitted cross section. Dashed lines give the level of QED cross section.

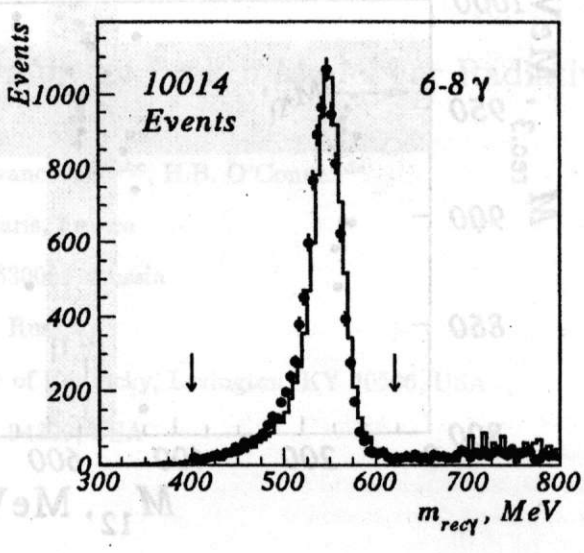

Figure 2. The recoil mass of the most energetic photon in an event. Points – data, histogram – simulation.

10 000. Fig. 2 shows the spectra of the recoil mass of most energetic photon ($M_{\rm rec}$) obtained from the data and the simulation. There is a good agreement in the spectra not only in the peak but also in the tail of the distribution, which is determined by the $e^+e^- \to K_S K_L$ background. This allows to estimate the contribution from background which does not exceed 1%. For final selection of $\eta\gamma$ events a soft cut 400 MeV $< M_{\rm rec} <$ 620 MeV was used.

The number of selected events in each energy point was fitted following the same approach as in the previous section. The main sources of systematic errors in this measurement are essentially the same. Using the table values of $B(\phi \to e^+e^-)$ and $B(\eta \to 3\pi^0)$ [15] the fitted value is

$$B(\phi \to \eta\gamma) = (1.296 \pm 0.024 \pm 0.057)\%. \qquad (5)$$

The small difference between this number and the published one [16] is due to the different model used to describe the interference of ρ and ω with ϕ meson.

Combining the result of this measurement with the result from the previous section we obtain the ratio of the decay widths of η in which some errors caused by the systematic effects cancel:

$$\frac{\Gamma(\eta \to 3\pi^0)}{\Gamma(\eta \to \gamma\gamma)} = 0.796 \pm 0.016 \pm 0.016. \qquad (6)$$

5. Decay $\phi \to \eta'\gamma \to \pi^+\pi^-\eta\gamma$

The decay $\phi \to \eta'\gamma$ is a long-searched process expected by many to clarify the question about the gluonium content of η'. The first observation of this decay was done at VEPP-2M in CMD-2 experiment [18]. The measurement of this decay at SND was performed with η' decaying into $\pi^+\pi^-\eta$ and η into two γ's. The features of this decay are the low energy of the recoil gamma, which makes it hard to measure reliably, and the big number and large cross sections of the background processes, which include $e^+e^- \to \eta\gamma \to \pi^+\pi^-\pi^0\gamma$, $e^+e^- \to \pi^+\pi^-\pi^0$, and $e^+e^- \to \omega\pi^0 \to \pi^+\pi^-\pi^0\pi^0$. For the analysis the events with two charged tracks and three photons were selected. To suppress the background a complex selection algorithm was developed based on the kinematics of all these processes. It was described in details in the ref. [19]. Due to the strict cuts, needed to suppress backgrounds, the selection efficiency for the events of the main process is only 5.5%. Fig. 3 shows the plot of recoil mass of the softest photon against the invariant mass of two other photons for all selected events.

The intersection of the shaded regions on the plot shows where the events of the decay $\phi \to \eta'\gamma$ should concentrate. We observe an excess of the events in this region with respect to what is expected from the background processes. This excess gives an estimate for $5.2^{+2.6}_{-2.2}$ events due to $\phi \to \eta'\gamma$ decay. It allows to conclude on the

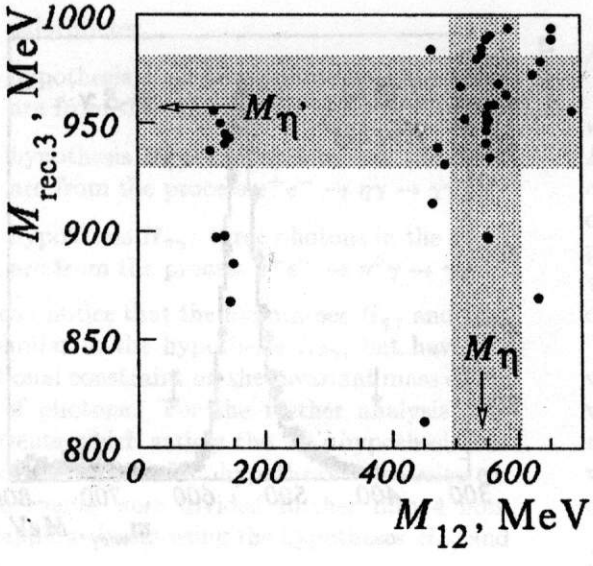

Figure 3. Plot of the recoil mass of the softest photon ($M_{\mathrm{rec},3}$) against the invariant mass of two other photons (M_{12}).

existence of the decay and obtain its branching ratio:

$$B(\phi \to \eta'\gamma) = (6.7^{+3.4}_{-2.9}) \times 10^{-5}. \qquad (7)$$

The systematic error, not included in the above errors, is about 15% and determined mainly by the error in the efficiency estimation.

6. Conclusion

The values $B(\phi \to \eta\gamma)$ and $B(\phi \to \pi^0\gamma)$ obtained at SND is one of the most precise measurements. Their precision is limited by the systematic effects – uncertainties in the $B(\phi \to e^+e^-)$ (3%), luminosity measurement (3%), error in the ϕ-meson phase determination in the OZI-suppressed $\phi \to \pi^0\gamma$ decay (6%). On the contrary, the measurement precision of $B(\phi \to \eta'\gamma)$ is limited by the available statistics and can be greatly improved by DAΦNE.

7. Acknowledgments

This work is partially supported by RFBR grant No. 96-15-96327 and STP "Integration" grant No. 274.

REFERENCES

1. L. Landsberg, Phys. Rep., 1985, vol. 128, p. 301.
2. P. O'Donnel, Rev. Mod. Phys., 1981, vol. 53, p. 673.
3. M. Benayoun et al., these proceedings.
4. E. Anashkin et al., ICFA Instr. Bull., 1988, vol. 5, p. 18.
5. V. Aulchenko et al., in Proc. Work. on Phys. and Detect. for DAΦNE (INFN, Frascati, 1991), p. 605.
6. M.N.Achasov et al., Preprint, BINP-99-16, Novosibirsk, 1999,
see also these proceedings.
7. S. Dolinsky et al., Phys. Rep., 1991, vol. 202, p. 99.
8. R. Akhmetshin et al., Phys. Lett. B, 1995, vol. 364, p. 199.
9. R.R.Akhmetshin et al, Physics Letters B, 1997, vol. 415, p. 445.
10. R.R.Akhmetshin et al, in Proc. ICHEP 98, 23-29 July 1998, Vancouver, Canada.
11. M.N. Achasov et al., Nucl. Instr. and Meth. A, 1998, vol. 411, p. 337.
12. M. Bekishev and V. Ivanchenko, Nucl. Instr. and Meth. A, 1995, vol. 361, p. 138.
13. E.A.Kurav and V.S.Fadin, Sov. J. Nucl. Phys., 1985, vol. 41, p. 466.
14. B. Geshkenbein and M. Terentyev, Jour. of Nucl. Phys., 1968, vol. 8, p. 550.
15. Particle Data Group, Eur. Phys. J. C, 1998, vol. 3.
16. M.N. Achasov et al., JETP Lett 1998, vol. 68, p. 573.
17. M.N.Achasov et al., Preprint BINP-97-78, 1997;
e-Print hep-ex/9710017;
in Proc. HADRON97, Upton, NY, August 24–30, 1997, pp.26–35.
18. R. Akhmetshin et al., Phys. Lett. B, 1997, vol. 415, p. 445.
19. V.M.Aulchenko et al., Pis'ma v ZhETF, 1999, vol. 69, p. 87.